



Deterministic Seismic Hazard Analysis to Determine Liquefaction Potential Due to Earthquake

K. A. Hanindya¹ , Lalu Makrup^{1*}, Widodo¹, R. Paulus²

¹ Department of Civil Engineering, Universitas Islam Indonesia, Yogyakarta, Indonesia.

² Department of Civil Engineering, Universitas Katholik Parahyangan, Bandung, Indonesia.

Received 13 February 2023; Revised 11 April 2023; Accepted 17 April 2023; Published 01 May 2023

Abstract

The great rocking of building structures and the occurrence of liquefaction in water-saturated soil on river banks are generally caused by earthquake shaking. The waves generated by the earthquake are the main cause of the shaking. In order to show the effect of ground motion earthquake shaking on the response of structures and liquefaction processes, it is necessary to analyze the structure and liquefaction as well as the time history of artificial earthquake ground motions. An artificial time history for liquefaction analysis can be developed based on spectral matching to the target spectrum generated by a deterministic seismic hazard analysis. Therefore, the time history recovered from the analysis can be said to be derived from a deterministic procedure. The analysis of liquefaction with time history aims to see the potential for liquefaction in the Palu region of Central Sulawesi by developing the time history of the bedrock. The time history of the bedrock is then spread over the ground surface. The propagation of time-historical waves to the ground surface can cause liquefaction events in the soil layer. It was found that liquefaction occurred in the Palu region, especially in the Anutapura Hospital building. No other liquefaction potential analysis studies were found in the region.

Keywords: Ground Motion; Time History; Seismic Hazard; Liquefaction Analysis.

1. Introduction

Sulawesi, in Central Indonesia (Figure 1), is an island located at the confluence of the Eurasian, Indo-Australian, and Pacific tectonic plates. These are complex areas where subduction and collision are still active. As a result of the shaking, the earthquake measuring 7.4 on the Richter scale, with the epicenter at a depth of 10 km, caused the phenomenon of liquefaction. The liquefaction phenomenon occurs in water-saturated, fine sandy soils. Identification of earthquake vibrations on the surface is very important to determine the possibility of liquefaction phenomena. In addition, earthquake vibration data on the ground surface is also needed to design high-rise buildings or other large-scale structures such as dams or bridges. Earthquake vibration data can be obtained from an earthquake recording station with an earthquake recording device called an accelerograph. The recording results in the form of ground vibration waves or also called earthquake ground motion waves. Generally, earthquake ground motion waves are actualized in the form of a time history of ground acceleration due to an earthquake, which is briefly referred to as "time history".

Installation of accelerographs to measure the time history of earthquake acceleration cannot be done everywhere due to limited resources. Therefore, there is a certain method to find the time history of earthquake acceleration. The method is Deterministic Seismic Hazard Analysis (DSHA), which involves Ground Motion Prediction Equations (GMPE) combined with a spectral matching method in the frequency domain to determine earthquake ground motion parameters

* Corresponding author: 885110106@uii.ac.id

 <http://dx.doi.org/10.28991/CEJ-2023-09-05-012>



© 2023 by the authors. Licensee C.E.J, Tehran, Iran. This article is an open access article distributed under the terms and conditions of the Creative Commons Attribution (CC-BY) license (<http://creativecommons.org/licenses/by/4.0/>).

in the form of earthquake acceleration time history. To see the potential for liquefaction in a place (for a certain point), the development of a time history of artificial earthquake acceleration must be carried out at a certain depth. An example is the soil layer at a depth of 30 meters from the ground surface.

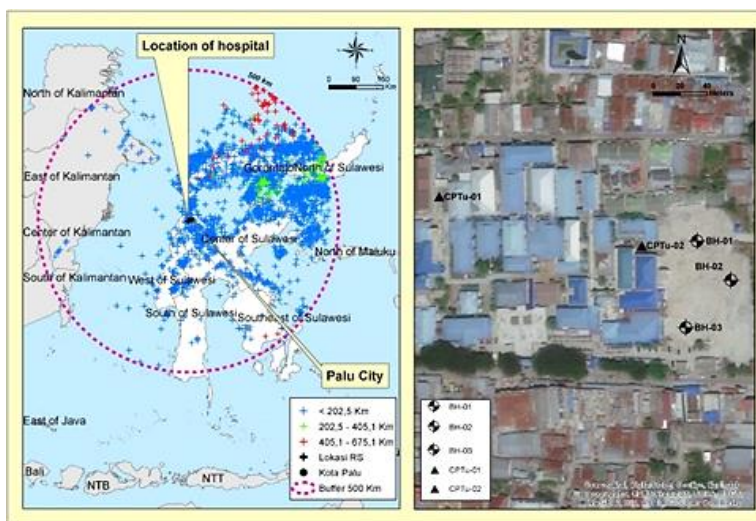


Figure 1. Location at BH01 and Palu Earthquake Data, Central Sulawesi, Indonesia

An example of the results of earthquake ground motion measurements in the form of the acceleration time history can be seen in Figure 2.

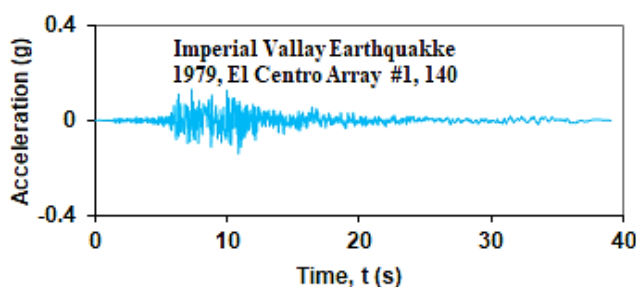


Figure 2. The acceleration time history result from the measurement of the 1979 Elcentro earthquake

It is assumed that at this depth, a rigid layer of soil or rock has been reached or is in accordance with the results of geological drilling. It is also assumed that the results of geological drilling have reached the rock layer. The development of the time history of artificial earthquake acceleration at rock depth aims to obtain earthquake waves in bedrock that can propagate to the ground surface with ground response analysis theory. The result of this analysis is to find the response of each soil layer in the form of acceleration. Along with soil response and geological drilling results, the liquefaction potential of each layer at the study site can be calculated.

2. Overview of Some Previous Research

Studies related to the development of earthquake acceleration waves in the form of acceleration time histories of the earthquake ground motion have been carried out by many experts. Pratiwi et al. [1] developed the ground motion time history to evaluate the displacement of dam structures in Java, Indonesia. Marzuko et al. [2] make artificial time histories to see the soil response to the frequency characteristic change of ground motion time histories. Erlangga et al. [3] evaluated the structure of the Law Faculty Building of the Islamic University of Indonesia Yogyakarta by applying the earthquake time history that they developed. Nicolaou [4] has carried out a study to develop acceleration time histories using the RASCAL computer program. Makrup [5] has made the computer program SPECMATCH to develop the earthquake's artificial acceleration time history based on the time history of the measurement result.

The acceleration time history result had a characteristic frequency that was different from the characteristic frequency of the earthquake acceleration measurement result (N4) [6]. Carlson et al. [7] developed the artificial acceleration time history based on 28 ground motions of the measurement result before using it as input to a bilinear SDOF system. Ergun and Ates [8] used time histories of measurement results to generate new time histories and compare the effects of near-fault ground motions on structures with far-fault ground motions' effects. Wood & Hutchinson [9] selected the ground motion using a probabilistic seismic hazard analysis and developed a new time history with a certain target spectrum. Bayati & Soltani [10] have selected the earthquake acceleration time history of the measurement result and, based on the time history, developed an artificial time history deterministically for the seismic design of RC frames against

collapse. Pavel & Vacareanu [11] selected the actual acceleration time history using a probabilistic seismic hazard analysis, and with a certain target spectrum, a new time history was generated. Makrup & Jamal [12] developed the artificial time history and design spectrum with probabilistic seismic hazard analysis and spectral matching in the time domain. Makrup [13] was driven to design ground motion with the probabilistic seismic hazard analysis and seismic code. Makrup & Muntafi [14] generated the artificial ground motion for the cities of Semarang and Solo, Indonesia, based on probabilistic seismic hazard analysis and spectral matching.

Related to the ground motion that can trigger the liquefaction, some authors have written papers about it. Subedi & Acharya [15] conducted the study to assess the liquefaction hazard in Kathmandu Valley. Kang et al. [16] made an assessment of the soil liquefaction potential using ambient noise. Fiitri & Pramana [17] did the liquefaction assessment based on grain size and CPT analysis. Bojadjieva et al. [18] made the study to Verification of a System for Sustainable Research on Earthquake-induced soil liquefaction in 1-g environments. Ahmad et al. [19] did an assessment of soil liquefaction potential in Kamra, Pakistan. Kim et al. [20] evaluated the post liquefaction volumetric strain of reconstituted samples based on soil compressibility. Sukkarak et al. [21] analyzed sandy soil liquefaction during a strong earthquake in northern Thailand. Kamura et al. [22] explored the possibility of assessing the degree of damage from liquefaction based only on seismic records using artificial neural networks. Jalil et al. [23] studied liquefaction in Palu as the cause of massive mudflows. Karastanev & Tchakalova [24] assessed the liquefaction potential of saturated loess. Uyanik [25] analyzed the soil liquefaction based on soil and earthquake parameters. Hashemi & Nikudel (2016) [26] made a study about the liquefaction potential that caused the earthquake based on CPT and N-SPT data. Agung et al. (2022) [27] carried out the analysis about the liquefaction potential level in Yogyakarta International Air Port. Lees et al. (2015) [28] made a study about the CPT-based analysis of liquefaction. Muntohar (2014) [29] did the research on earthquake-induced liquefaction in Padang and Yogyakarta, Indonesia.

In this research, the earthquake artificial acceleration time history in base rock will be developed based on the deterministic seismic hazard analysis, and then the time history will be propagated to the ground surface to see the liquefaction potential of each soil layer.

3. Research Methodology

Tatsuoka et al. (1980) [30] evaluated the potential for soil liquefaction based on SPT. Meanwhile, Seed and Idriss (1971) [31] have proven suitable and can be used for liquefaction assessment. So that the liquefaction potential is determined and carried out based on the following Figure 3.

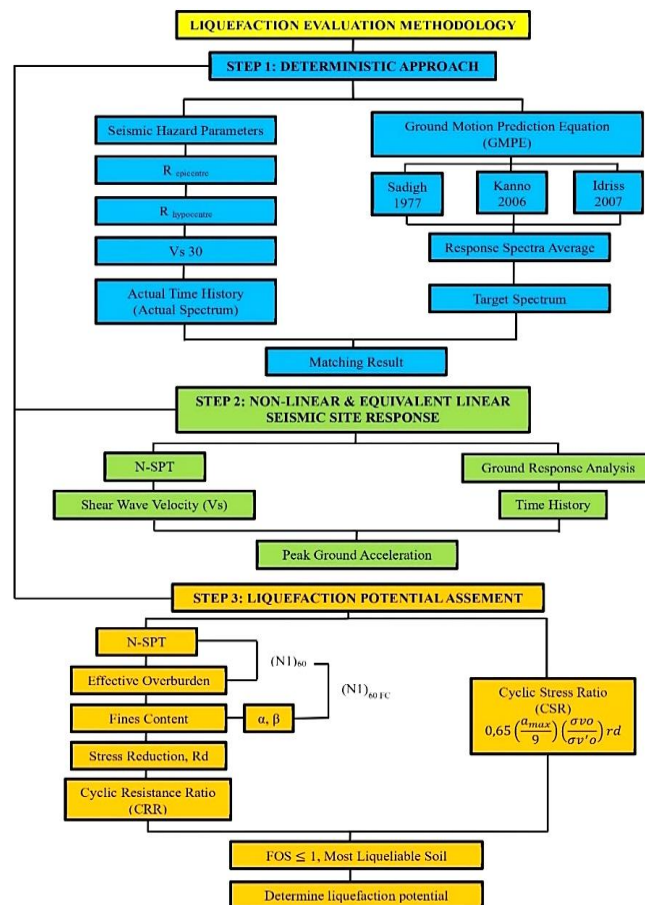


Figure 3. Deterministic Approach to Determine Liquefaction Potential Methodology

4. Deterministic Seismic Hazard Analysis

The development of earthquake ground motion by probabilistic procedures has been carried out by many experts. Another procedure for developing earthquake ground motion is a deterministic seismic hazard analysis. To develop a deterministic earthquake, ground motion is used as a basis for the Ground Motion Prediction Equation (GMPE). There are quite a number of GMPEs developed by experts, but in this study only three GMPEs were used as a reference to accommodate the causes of uncertainty by using one GPME. There are quite a number of GMPEs developed by experts, but in this study only three GMPEs were used as a reference to accommodate the causes of uncertainty by using one GPME. Because what is calculated or developed is the ground motion in the bedrock, the GMPE used is the GMPE of rock sites. The computational result of each GPME is the response spectrum of the bedrock. In this study, three GMPEs will be used, namely Sadigh et al. (1997) [32], Idriss (2007) [33], and Kanno et al. (2006) [34]. Why are these three GMPEs used in research? Because these three equations have input data that can still be found in Indonesia. The average value of the response spectra of the three GMPEs above will be used as a target spectrum to develop an artificial time history. The mathematical equations of Sadigh et al. (1997) [32], Idriss (2007) [33], and Kanno et al. (2006) [34] are presented below.

Sadigh equation (1997) [32] for rock.

$$\ln Y = C1 + C2 M + C3 (8.5 - M)^{2.5} + C4 \ln[RRUP + \exp(C5 + C6 M)] + C7 \ln[RRUP + 2] \quad (1)$$

Sadigh equation (1997) [32] for soil.

$$\ln y = C1 + C2 M + C3 \ln[RRUP + C4 e^{C5 M}] + C6 + C7 (8.5 - M)^{2.5} \quad (2)$$

where, y = spectral acceleration, M = earthquake magnitude ($M = 4$ to 8), $RRUP$ = rupture distance ($RRUP = 0$ to 100 km), and regression coefficients $C1$ to $C7$.

Idriss equation (2007) [33].

$$\ln PAA(g) = \alpha_1 + \alpha_2 M - (\beta_1 + \beta_2 M) \ln(RRUP + 10) + \gamma RRUP + \phi F \quad (3)$$

where, PAA is pseudo-absolut-spectral acceleration, M is earthquake magnitude, $RRUP$ is rupture distance, γ is approach distance factor, ϕ is source mechanism factor, F is source mechanism ($F = 0$ for strike slip faulting and $F = 1$ for reverse faulting), and α_1 , α_2 , β_1 , β_2 are regression parameters.

Kanno equation (2006) [34].

$$\log y = a_1 M + b_2 RRUP - \log(RRUP + c_1 + c_4 100.5 M) + p \log VS30 + q \quad (4)$$

Equation 4 gives the result y in cm/s^2 . If y is in the acceleration due to gravity, then Equation 4 turns into Equation 5.

$$\ln y = \ln(10) \log y - \ln(100g) \quad (5)$$

where, y is ground motion parameter, M is earthquake magnitude, $RRUP$ is rupture distance, a_1 , b_2 , c_1 , c_4 , p and q are regression coefficients.

4.1. Target Spectrum Determination

The target spectrum is developed based on the ground motion prediction equation, namely Sadigh et al. (1997) [32], Idriss (2007) [33], and Kanno et al. (2006) [34]. The third GMPE uses the rupture distance parameter to calculate the acceleration of ground motion. However, at the location of the case study, only the epicenter (R_{epi}) and hypocenter (R_{hipo}) distances are available. Therefore, the rupture distance is replaced by the hypocenter distance. The research location is the Palu earthquake, September 2018, with global coordinates of -0.90007 south and $119,84918$ east. The coordinates are: Anutapura Hospital Palu, Central Sulawesi, Indonesia. The magnitude (M) and distance of the hypocenter (R) of the earthquake are $M = 7.4$ and $R = 80.911$ km.

The results of the calculation of response spectra on bedrock with $M = 7.4$ and $R = 80.911$ km using GMPE from Sadigh et al. (1997) [32] can be seen in Figure 4.

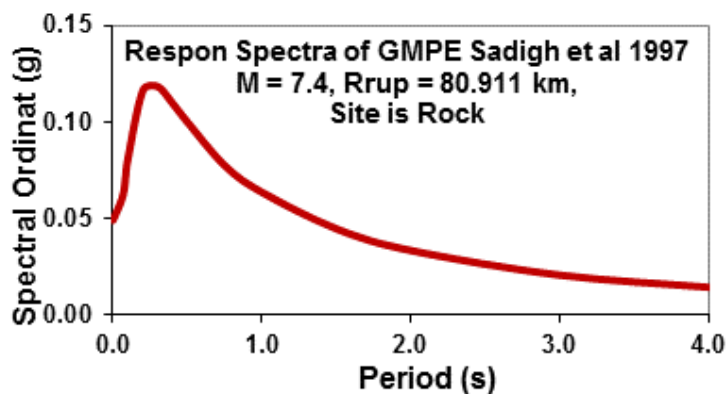


Figure 4. GMPE response spectra of Sadigh et al. (1997) [32]

The results of the bedrock response spectrum used by GMPE Idriss (2007) based on M and R above are in Figure 5.

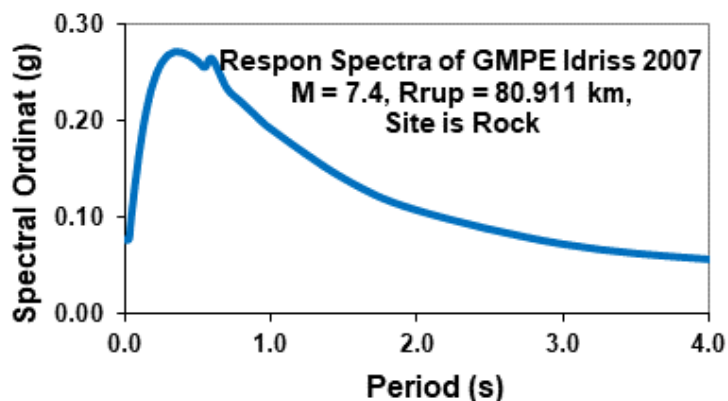


Figure 5. GMPE response spectra of Idriss (2007) [33]

The result of the response spectra in bedrock used by GMPE of Kanno et al. (2006) [34] with M and R above are in Figure 6. The average values of the response spectra of Figures 4 to 7.

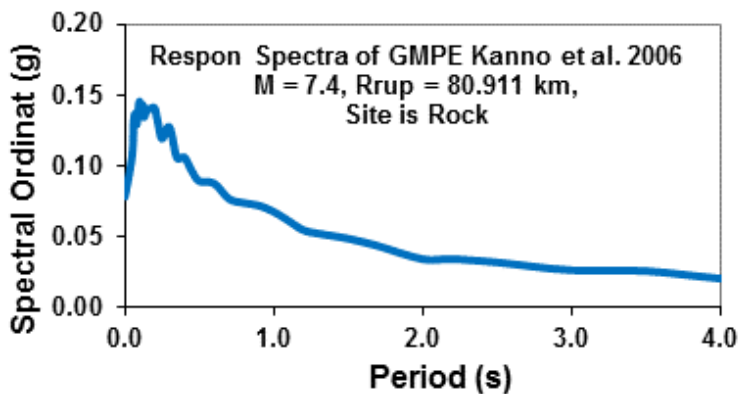


Figure 6. GMPE response spectra of Kanno et al. (2006) [34]

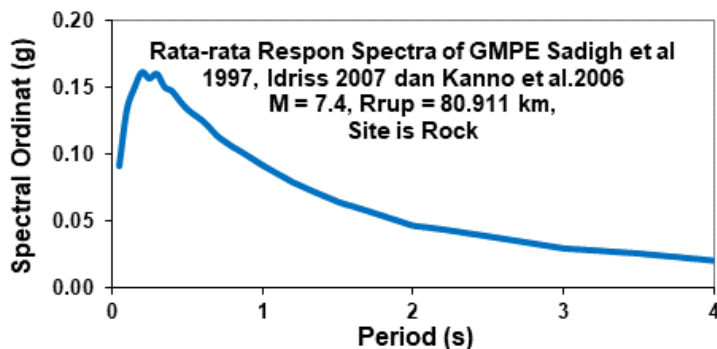


Figure 7. The average value of the response spectrum Sadigh et al (1997) [32], Idriss (2007) [33] and Kanno et al. (2006) [34]

In this case, it is stated that the target spectrum is a response spectrum that is developed deterministically and is the response spectrum of Figure 7.

4.2. Actual Time History

The target spectrum is developed based on the ground motion prediction equation, namely Sadigh et al. (1997) [32]. Another basis for determining the time history of artificial earthquake ground acceleration is the result of measuring the time history, which is called the actual time history. For this study, the Mammoth Lakes-06, 27/5/1980, Bishop-Paradise Lodge, 70, USA earthquake will be used as real-time history. This time history can be seen in Figure 8.

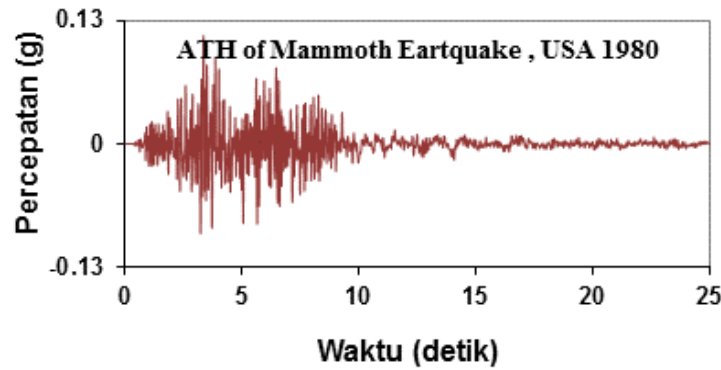


Figure 8. Mammoth Lake time history-06, 1980, Paradise Lodge, USA

4.3. Matching Result

The target spectrum is developed based on the ground motion prediction equation, namely Sadigh et al. (1997) [32]. Another basis for determining the result of the spectral match between the actual response spectrum of Figure 9 and the target spectrum of Figure 7 is the combined response spectrum of Figure 10, and the other result is the time history of Figure 11.

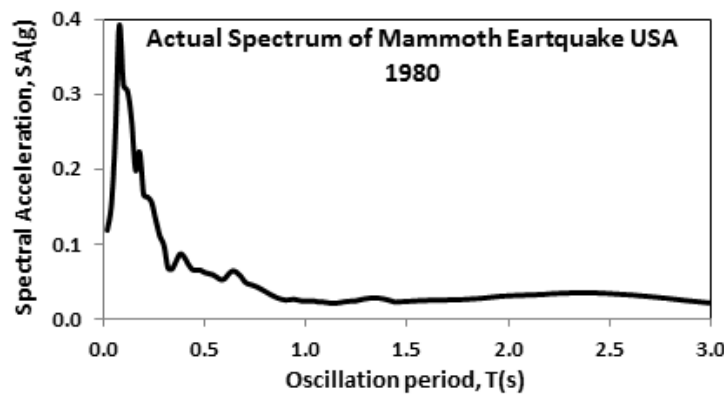


Figure 9. Actual response spectrum from time history Figure 6

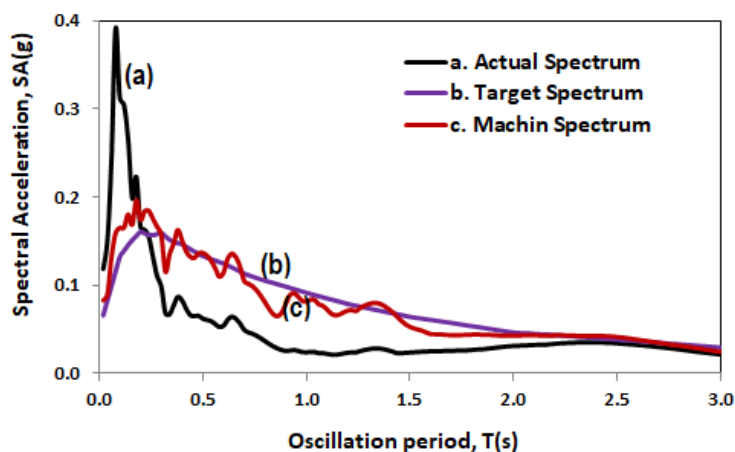


Figure 10. The results of the spectral matching of the response spectra between the response spectra of Figure 9 to Figure 7

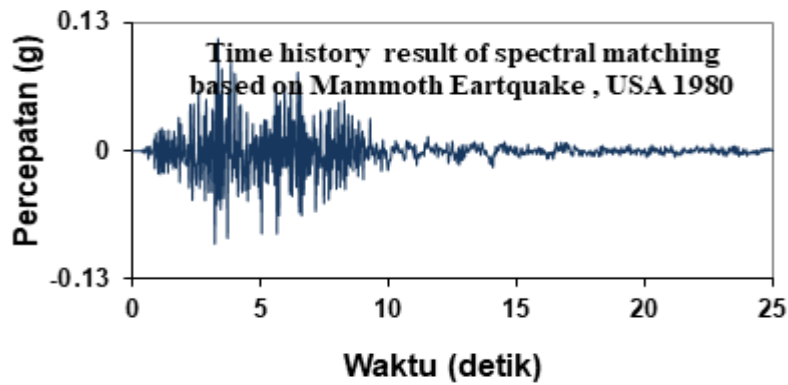


Figure 11. The time history of the spectral match results between the response spectrum of Figure 9 and the response spectrum of Figure 7

Time history Figure 9 is an artificial time history in bedrock. Time history is said to have been developed by Deterministic Seismic Hazard Analysis (DSHA) because the target spectrum used to develop this time history was developed by DSHA.

5. Earthquake Wave Propagation

The earthquake wave referred to here is the acceleration time history of an earthquake, which is recorded on a site. To propagate earthquake waves from the bedrock to the soil surface, data on the properties of the soil layers is needed. These properties can be discovered by soil investigation in the form of geological drilling. In this case, the results of the drilling at Anutapura Hospital Palu can be seen in Figure 12. Figure 12a shows the relationship between the Normal Penetration Test (N-SPT) and depth and time. The N-SPT is converted to the ground shear wave velocity (V_s) in Figure 12b. The calculation of V_s was carried out by the formula of Oshima et al. (2001) [35] and by Imai and Tonouchi (2021) [36]. The formula is in Equations 6 and 7.

$$V_s = 85.3 N^{0.341} \tag{6}$$

$$V_s = 96.9 N^{0.314} \tag{7}$$

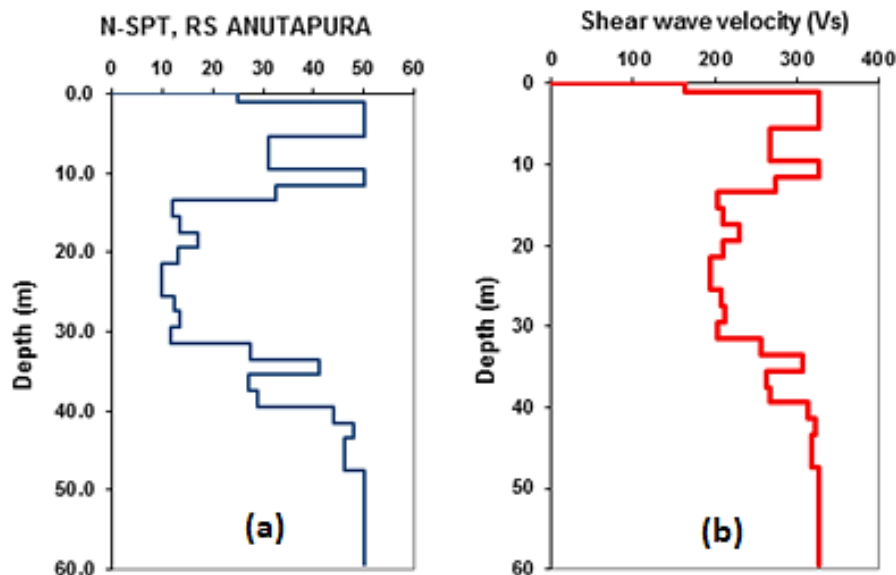


Figure 12. The results of the soil investigation is as a geological drilling results in form N-SPT versus depth and time at Anutapura Hospital, Palu location

Using soil shear wave velocity data (Figure 12-b) and theoretical soil response analysis, the time history of Figure 11 can be propagated from bedrock to the soil surface with DEEPSOIL software. The results of the propagation of time history are shown in Figure 13. Time history of propagation: Figure 13 will be used to determine the potential for liquefaction at the Anutapura Hospital Palu location. The results of the propagation time history are shown in Figure 13. The propagation time history in Figure 13 will be used to determine the potential for liquefaction at the Anutapura Hospital Palu location.

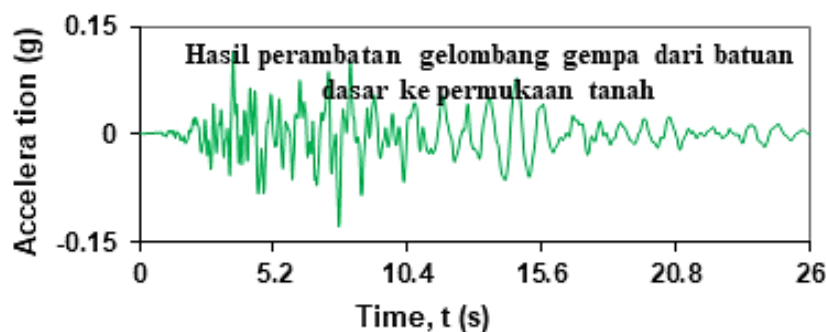


Figure 13. Time history of propagation result from bedrock to soil surface

6. Determination of Liquefaction Potential

Liquefaction is a phenomenon in which the strength and stiffness of a soil are reduced by earthquake shaking, so that the soil behaves as liquid. The determination of the liquefaction potential was carried out at the Anutapura Hospital Palu location with a total of 30 layers of soil (Figure 12). From the time history in Figure 13, it is found that the maximum acceleration (a_{max}) = 0.1292g. Together with a_{max} = 0.1292g and the magnitude of the Palu earthquake in September 2018 with $M = 7.4$, liquefaction potential can be calculated based on the simplified seed method.

The parameters needed to determine the liquefaction potential depend on G_s (specific gravity), e (pore number), and γ_d (dry soil volume weight) and are contained in the following equation.

$$\gamma_d = \frac{G_s \gamma_w}{1+e} \quad (8)$$

while the saturated soil volume weight γ_d is formulated as follows.

$$\gamma_{sat} = \frac{(G_s+e)\gamma_w}{1+e} \quad (9)$$

while the dry soil volume weight γ is formulated as follows.

$$\gamma' = \gamma_{sat} - 1 \quad (10)$$

while the vertical normal stress for the pure soil σ_v is formulated as follows.

$$\sigma_v = \gamma h \quad (11)$$

while the vertical normal stress for dry soil σ'_v is formulated as follows.

$$\sigma'_v = \gamma' h \quad (12)$$

Function and curve for determining liquefaction potential with simplified Seed method are:

a. Stress reduction factor

$$r_d = \frac{1-0.4113z^{0.5}+0.04052z+0.001753z^{1.5}}{1-0.4177z^{0.5}+0.05729z-0.006205z^{1.5}+0.00121z^2} \quad (13)$$

b. Cyclic stress ratio

$$CSR = \frac{\tau_{av}}{\sigma'_v} = 0.65 \frac{a_{max}}{g \frac{\sigma_v}{\sigma'_v}} \quad (14)$$

c. N-SPT correction factor

$$C_N = 1 - 1.25 \log \frac{\sigma'_v}{10.76391} \quad (15)$$

d. N' is corrected N

$$N' = C_N N\text{-SPT} \quad (16)$$

e. Relative density

$$D_r = \sqrt{\frac{N}{2.417965\sigma_v+17}} \quad (17)$$

f. Vertical shear stress ratio and vertical stress the dry soil and also known as cyclic stress ratio gave by Seed and Idriss in form of:

$$\frac{\tau_{av}}{\sigma'_v} = 0.65 \frac{a_{max}}{g} \frac{\sigma_v}{\sigma'_v} r_d \quad (18)$$

r_d value can be calculated based on Equation 13 or can be determined with the curve Figure 14.

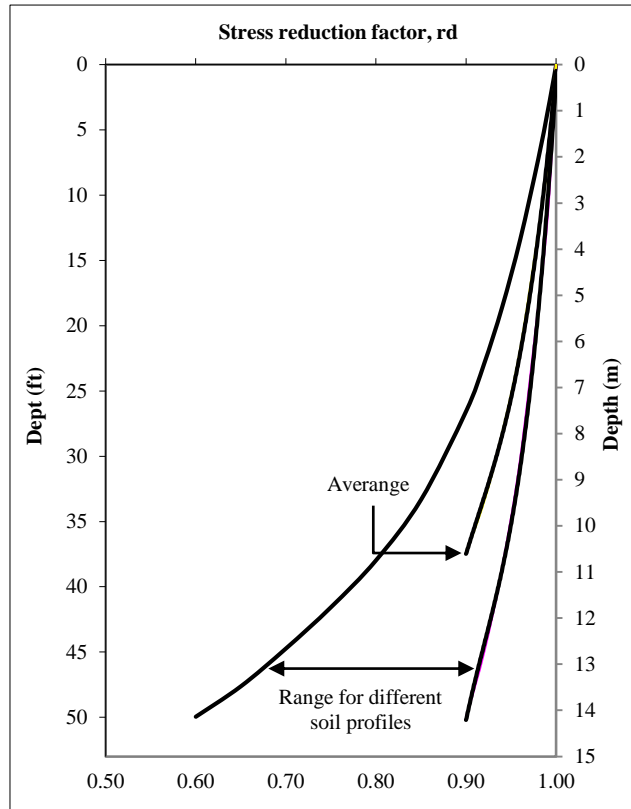


Figure 14. Curve to determine r_d value, Equation 13

The liquefaction potential can be determine based on the Figure 15 curve. The curve developed by Seed and Idriss based on soil cyclic stress ratio and corrected normal-penetration tes (N').

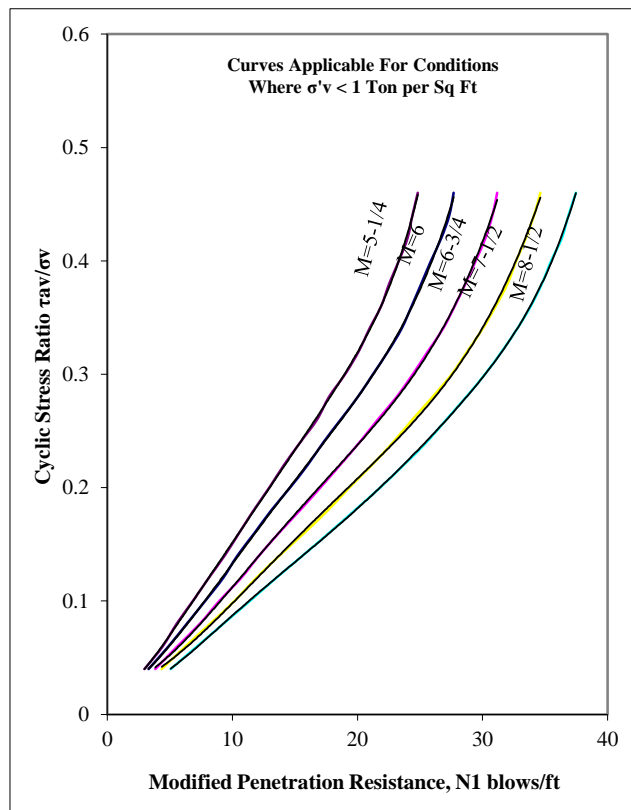


Figure 15. Curve to determine the liquefaction potential

Table 1. Calculation of vertical soil stress (σ_v and σ_v')

Depth (m)	γ_{sat} (ton/m ³)	γ' (ton/m ³)	γ_d (ton/m ³)	σ_v' (ton/m ²)	σ_v (ton/m ²)	σ_v/σ_v'
1.11	-	-	1.444	1.603	1.603	1.000
3.45	-	-	1.456	5.010	5.010	1.000
5.45	1.889	0.889	-	6.788	8.788	1.295
7.45	1.889	0.889	-	8.566	12.566	1.467
9.45	1.889	0.889	-	10.344	16.344	1.580
11.45	1.889	0.889	-	12.122	20.122	1.660
13.45	1.889	0.889	-	13.900	23.900	1.719
15.45	1.889	0.889	-	15.678	27.678	1.765
17.45	1.889	0.889	-	17.456	31.456	1.802
19.45	1.889	0.889	-	19.234	35.234	1.832
21.45	1.889	0.889	-	21.012	39.012	1.857
23.45	1.889	0.889	-	22.790	42.790	1.878
25.45	1.889	0.889	-	24.568	46.568	1.895
27.45	1.889	0.889	-	26.346	50.346	1.911
29.45	1.889	0.889	-	28.124	54.124	1.924
31.45	1.889	0.889	-	29.902	57.902	1.936
33.45	1.889	0.889	-	31.680	61.680	1.947
35.45	1.889	0.889	-	33.458	65.458	1.956
37.45	1.889	0.889	-	35.236	69.236	1.965
39.45	1.889	0.889	-	37.014	73.014	1.973
41.45	1.889	0.889	-	38.792	76.792	1.980
43.10	1.889	0.889	-	40.259	79.909	1.985
45.05	1.889	0.889	-	41.992	83.592	1.991
47.39	1.889	0.889	-	44.073	88.013	1.997
49.40	1.889	0.889	-	45.859	91.809	2.002
51.15	1.889	0.889	-	47.415	95.115	2.006
53.10	1.889	0.889	-	49.149	98.799	2.010
55.15	1.889	0.889	-	50.971	102.671	2.014
57.10	1.889	0.889	-	52.705	106.355	2.018
59.05	1.889	0.889	-	54.438	110.038	2.021

7. Liquefaction Calculation

The calculation for determining the liquefaction potential at the soil layers at the Anutapura hospital is computed based on the earthquake maximum acceleration (a_{max}) = 0.1292g at the ground surface and the N-SPT value of the soil layers (Figure 12-a). The first is calculated as the vertical stress for the saturated soil (s_v) and the vertical stress for the waterlogged soil ($s_v\phi$). Based on the cyclic stress ratio ($t_{av}/s_v\phi$) and modified penetration resistance (N') in Figure 15, the liquefaction potential can be determined as in Table 2. However, Seed & Idriss (1971) [31] and a vast number of past experiences have shown that liquefaction seldom occurs at depths larger than about 20 m.

In column 10 of Table 2 and from Figure 16 the liquefaction state of the letter L occurs and the letter NL does not occur. From the Table 2 can be stated: the soil layer 1 and 2 liquefaction are not occurred, layer 3 to 6 are occurred, layer 7 is not occurred, layer 8 is occurred, layer 9 are not occurred, layer 10 is occurred, and layer 11 to 30 are not occurred because.

Table 2. Liquefaction potential calculation

Soil layer	Depth (m)	σ_v/σ'_v	N-SPT value	Dr	CN	N'	R _d	τ_{av}/σ'_v	NL/L
1	1.11	1.000	50	2.3951	2.0338	101.6925	0.9934	0.0834	NL
2	3.45	1.000	17	0.5839	1.4152	24.0580	0.9764	0.0820	NL
3	5.45	1.295	4	0.1046	1.2503	5.0012	0.9621	0.1046	L
4	7.45	1.467	8	0.1688	1.1240	8.9920	0.9438	0.1163	L
5	9.45	1.580	10	0.1769	1.0216	10.2161	0.9153	0.1215	L
6	11.45	1.660	11	0.1675	0.9355	10.2905	0.8715	0.1215	L
7	13.45	1.719	14	0.1872	0.8612	12.0568	0.8123	0.1173	NL
8	15.45	1.765	27	0.3217	0.7959	21.4880	0.7457	0.1106	L
9	17.45	1.802	25	0.2686	0.7375	18.4384	0.6827	0.1033	NL
10	19.45	1.832	12	0.1174	0.6849	8.2185	0.6303	0.0970	L
11	21.45	1.857	20	0.1796	0.6369	12.7376	0.5899	0.0920	NL
12	23.45	1.878	6	0.0498	0.5928	3.5567	0.5596	0.0882	NL
13	25.45	1.895	12	0.0926	0.5520	6.6240	0.5368	0.0855	NL
14	27.45	1.911	9	0.0649	0.5141	4.6266	0.5191	0.0833	NL
15	29.45	1.924	10	0.0676	0.4786	4.7862	0.5049	0.0816	NL
16	31.45	1.936	6	0.0382	0.4453	2.6720	0.4930	0.0802	NL
17	33.45	1.947	17	0.1023	0.4140	7.0377	0.4828	0.0789	NL
18	35.45	1.956	19	0.1084	0.3843	7.3025	0.4737	0.0778	NL
19	37.45	1.965	11	0.0596	0.3562	3.9185	0.4654	0.0768	NL
20	39.45	1.973	9	0.0465	0.3295	2.9656	0.4577	0.0758	NL
21	41.45	1.980	16	0.0789	0.3040	4.8646	0.4505	0.0749	NL
22	43.10	1.985	50	0.2379	0.2839	14.1944	0.4448	0.0741	NL
23	45.05	1.991	50	0.2282	0.2610	13.0500	0.4384	0.0733	NL
24	47.39	1.997	50	0.2176	0.2348	11.7376	0.4311	0.0723	NL
25	49.40	2.002	50	0.2092	0.2132	10.6588	0.4251	0.0715	NL
26	51.15	2.006	50	0.2024	0.1951	9.7533	0.4200	0.0708	NL
27	53.10	2.010	50	0.1954	0.1756	8.7786	0.4145	0.0700	NL
28	55.15	2.014	50	0.1885	0.1558	7.7903	0.4089	0.0692	NL
29	57.10	2.018	50	0.1824	0.1377	6.8825	0.4038	0.0684	NL
30	59.05	2.021	50	0.1766	0.1201	6.0041	0.3988	0.0677	NL

Note: NL (Non-Liquefiable Soil); L (Liquefiable Soil)

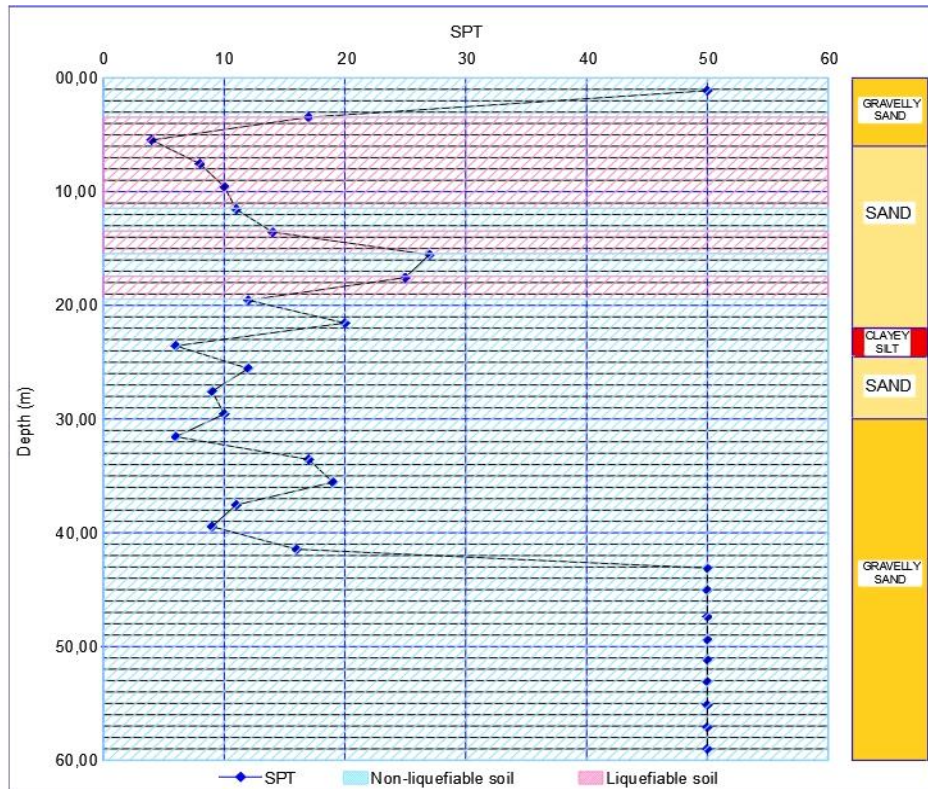


Figure 16. Result of liquefaction potential

8. Conclusion and Recommendation

The research has produced the ground motion in the bedrock caused by the earthquake, which is called the time history of earthquake acceleration ground motion. The bedrock time history is then propagated to the ground surface and called the surface time history. The maximum value of the surface time history is then used as the basis to determine the liquefaction potential together with the normal-penetration test value at the point of the Anutapura hospital, Palu Central Sulawesi. From the calculation result, it was found that at the Anutapura hospital, liquefaction occurred at the soft soil, and at the stiff soil, liquefaction was possible but did not occur because liquefaction seldom occurs at depths larger than about 20 m.

The study of the liquefaction potential based on the earthquake wave propagation from bedrock to the ground surface can still be carried out at other places. Therefore, my colleague's interest in carrying out research about liquefaction can start from now.

9. Declarations

9.1. Author Contributions

Conceptualization, K.A.H., L.M., W., and R.P.; methodology, K.A.H. and L.M.; data curation, W., and R.P.; writing—original draft preparation, K.A.H., L.M., W., and R.P.; writing—review and editing, K.A.H., L.M., W., and R.P. All authors have read and agreed to the published version of the manuscript.

9.2. Data Availability Statement

The data presented in this study are available in the article.

9.3. Funding

The authors received no financial support for the research, authorship, and/or publication of this article.

9.4. Conflicts of Interest

The authors declare no conflict of interest.

10. References

- [1] Pratiwi, D. A. W. W., Makrup, L., & Setiawan, I. (2022). The Structural Dynamic Evaluation of Wadasintang Dam to the Earthquake Acceleration Based on Indonesian Seismic Code 2019. *American Journal of Civil Engineering*, 10(3), 125-134. doi:10.11648/j.ajce.20221003.15.
- [2] Marzuko, A., Makrup, L., Abdurrazak, M. R. (2022). The Effect of the Soil Response to the Change of the Frequency Characteristic of the Earthquake Ground Motions, *American Journal of Civil Engineering*. 10(4), 145-152. doi:10.11648/j.ajce.20221004.11.
- [3] Erlangga, W., Makrup, L., Mushthofa, M., & Suharyatmo, D. (2022) Evaluation of Law Faculty Building of Islamic University of Indonesia based on earthquake acceleration was determined with probabilistic concept. *Teknisia*, 27, 1. (In Indonesian).
- [4] Nikolaou, A. S. (1998). A GIS platform for earthquake risk analysis. Ph.D. Thesis, State University of New York, Buffalo, United States.
- [5] Makrup, L. (2017). Change the frequency characteristics of the earthquake acceleration wave by Fourier analysis. *International Journal of Civil Engineering and Technology*, 8(12), 1045–1055.
- [6] Saputra, E., Nugraheni, F., Pawirodikromo, W., & Makrup, L. (2021). Comparison of Soil Surface Seismic Hazard Maps as Basic Disaster Mitigation Based Spatial Planning in Riau Province. *Media Komunikasi Teknik Sipil*, 27(2), 250–259. doi:10.14710/mkts.v27i2.36902.
- [7] Carlson, C. P., Zekkos, D., & McCormick, J. P. (2014). Impact of time and frequency domain ground motion modification on the response of a SDOF system. *Earthquake and Structures*, 7(6), 1283–1301. doi:10.12989/eas.2014.7.6.1283.
- [8] Ergun, M., & Ates, S. (2013). Selecting and scaling ground motion time histories according to Eurocode 8 and ASCE 7-05. *Earthquake and Structures*, 5(2), 129–142. doi:10.12989/eas.2013.5.2.129.
- [9] Wood, R. L., & Hutchinson, T. C. (2012). Effects of ground motion scaling on nonlinear higher mode building response. *Earthquake and Structures*, 3(6), 869–887. doi:10.12989/eas.2012.3.6.869.
- [10] Bayati, Z., & Soltani, M. (2016). Ground motion selection and scaling for seismic design of RC frames against collapse. *Earthquake and Structures*, 11(3), 445–459. doi:10.12989/eas.2016.11.3.445.

- [11] Pavel, F., & Vacareanu, R. (2016). Scaling of ground motions from Vrancea (Romania) earthquakes. *Earthquakes and Structures*, 11(3), 505–516. doi:10.12989/eas.2016.11.3.505.
- [12] Makrup, L., & Jamal, A.U. (2016). The Earthquake Ground Motion and Response Spectra Design for Sleman, Yogyakarta, Indonesia with Probabilistic Seismic Hazard Analysis and Spectral Matching in Time Domain. *American Journal of Civil Engineering*, 4(6), 298. doi:10.11648/j.ajce.20160406.15.
- [13] Makrup, L. (2017). Generating Design Ground Motion by Probabilistic Seismic Hazard Analysis and Code. *Electronic journal of Geotechnical Engineering*, 22, 1567-1586.
- [14] Makrup, L., & Muntafi, Y. (2016). Artificial ground motion for the cities of Semarang and solo Indonesia generated based on probabilistic seismic hazard analysis and spectral matching. *Electronic Journal of Geotechnical Engineering*, 21(21), 6587–6602.
- [15] Subedi, M., & Acharya, I. P. (2022). Liquefaction hazard assessment and ground failure probability analysis in the Kathmandu Valley of Nepal. *Geoenvironmental Disasters*, 9(1). doi:10.1186/s40677-021-00203-0.
- [16] Kang, S. Y., Kim, K. H., Gihm, Y. S., & Kim, B. (2022). Soil liquefaction potential assessment using ambient noise: A case study in Pohang, Korea. *Frontiers in Earth Science*, 10, 2022. doi:10.3389/feart.2022.1029996.
- [17] Nurlita Fitri, S., & Wahyu Pramana, I. M. (2022). Liquefaction Assessment Based on Grain Size and CPT Analysis for Birobuli Area, South Palu. *Teknisia*, 27(2), 95–102. doi:10.20885/teknisia.vol27.iss2.art3.
- [18] Bojadjeva, J., Sheshov, V., Edip, K., & Kitanovski, T. (2022). Verification of a System for Sustainable Research on Earthquake-Induced Soil Liquefaction in 1-g Environments. *Geosciences (Switzerland)*, 12(10), 363. doi:10.3390/geosciences12100363.
- [19] Ahmad, M., Tang, X. W., Ahmad, F., & Jamal, A. (2018). Assessment of soil liquefaction potential in Kamra, Pakistan. *Sustainability (Switzerland)*, 10(11), 4223. doi:10.3390/su10114223.
- [20] Kim, J., Kazama, M., & Kawai, T. (2021). Evaluation of post-liquefaction volumetric strain of reconstituted samples based on soil compressibility. *Soils and Foundations*, 61(6), 1555–1564. doi:10.1016/j.sandf.2021.09.002.
- [21] Sukkarak, R., Tanapalungkorn, W., Likitlersuang, S., & Ueda, K. (2021). Liquefaction analysis of sandy soil during strong earthquake in Northern Thailand. *Soils and Foundations*, 61(5), 1302–1318. doi:10.1016/j.sandf.2021.07.003.
- [22] Kamura, A., Kurihara, G., Mori, T., Kazama, M., Kwon, Y., Kim, J., & Han, J. T. (2021). Exploring the possibility of assessing the damage degree of liquefaction based only on seismic records by artificial neural networks. *Soils and Foundations*, 61(3), 658–674. doi:10.1016/j.sandf.2021.01.014.
- [23] Jalil, A., Fathani, T. F., Satyarno, I., & Wilopo, W. (2021). Liquefaction in Palu: the cause of massive mudflows. *Geoenvironmental Disasters*, 8(1). doi:10.1186/s40677-021-00194-y.
- [24] Karastanev, D., & Tchakalova, B. (2021). Liquefaction potential assessment of saturated loess. *Geologica Balcanica*, 50(1), 37–44. doi:10.52321/GeolBalc.50.1.37.
- [25] Uyanık, O. (2020). Soil liquefaction analysis based on soil and earthquake parameters. *Journal of Applied Geophysics*, 176, 104004. doi:10.1016/j.jappgeo.2020.104004.
- [26] Hashemi, M., & Nikudel, M. R. (2016). Application of dynamic cone penetrometer test for assessment of liquefaction potential. *Engineering Geology*, 208, 51-62. doi:10.1016/j.enggeo.2016.04.013.
- [27] Agung, P. A. M., Ahmad, M. A., & Hasan, M. F. R. (2022). Probability Liquefaction On Silty Sand Layer On Central Jakarta. *International Journal of Integrated Engineering*, 14(9), 48-55.
- [28] Lees, J. J., Ballagh, R. H., Orense, R. P., & van Ballegooy, S. (2015). CPT-based analysis of liquefaction and re-liquefaction following the Canterbury earthquake sequence. *Soil Dynamics and Earthquake Engineering*, 79, 304–314. doi:10.1016/j.soildyn.2015.02.004.
- [29] Muntohar, A. S. (2014). Research on earthquake induced liquefaction in Padang City and Yogyakarta area. *Jurnal Geoteknik HATTI IX*, 1, 0853-4810.
- [30] Tatsuoka, F., Iwasaki, T., Tokida, K.-I., Yasuda, S., Hirose, M., Imai, T., & Kon-No, M. (1980). Standard Penetration Tests and Soil Liquefaction Potential Evaluation. *Soils and Foundations*, 20(4), 95–111. doi:10.3208/sandf1972.20.4_95.
- [31] Seed, H. B., & Idriss, I. M. (1971). Simplified Procedure for Evaluating Soil Liquefaction Potential. *Journal of the Soil Mechanics and Foundations Division*, 97(9), 1249–1273. doi:10.1061/jsfeaq.0001662.
- [32] Sadigh, K., Chang, C.-Y., Egan, J. A., Makdisi, F., & Youngs, R. R. (1997). Attenuation Relationships for Shallow Crustal Earthquakes Based on California Strong Motion Data. *Seismological Research Letters*, 68(1), 180–189. doi:10.1785/gssrl.68.1.180.
- [33] Boulanger, R. W., & Idriss, I. M. (2007). Evaluation of Cyclic Softening in Silts and Clays. *Journal of Geotechnical and Geoenvironmental Engineering*, 133(6), 641–652. doi:10.1061/(asce)1090-0241(2007)133:6(641).

- [34] Kanno, T., Narita, A., Morikawa, N., Fujiwara, H., & Fukushima, Y. (2006). A New Attenuation Relation for Strong Ground Motion in Japan Based on Recorded Data. *Bulletin of the Seismological Society of America*, 96(3), 879–897. doi:10.1785/0120050138.
- [35] Oshima, T., Yamamoto, T., Ohto, K., Goto, M., Nakashio, F., & Furusaki, S. (2001). A calixarene-based phosphoric acid extractant for rare earth separation. *Solvent Extraction Research and Development*, 2001(8), 194-204.
- [36] Imai, T., & Tonoughi, K. (2021). Correlation of N value with S-wave velocity and shear modulus. *Penetration Testing*, 67-72. Routledge, Taylor & Francis, New York, United States.